Photocontrolling Protein–Peptide Interactions: From Minimal Perturbation to Complete Unbinding

Jankovic, Brankica ; Gulzar, Adnan ; Zanobini, Claudio ; Bozovic, Olga ; Wolf, Steffen ; Stock, Gerhard ; Hamm, Peter

Abstract: An azobenzene-derived photoswitch has been covalently cross-linked to two sites of the S-peptide in the RNase S complex in a manner that the alpha-helical content of the S-peptide reduces upon cis-to-trans isomerization of the photoswitch. Three complementary experimental techniques have been employed, isothermal titration calorimetry, circular dichroism spectroscopy and intrinsic tyrosine fluorescence quenching, to determine the binding affinity of the S-peptide to the S-protein in the two states of the photoswitch. Five mutants with the photoswitch attached to different sites of the S-peptide have been explored, with the goal to maximize the change in binding affinity upon photoswitching, and to identify the mechanisms that determine the binding affinity. With regard to the first goal, one mutant has been identified, which binds with reasonable affinity in the one state of the photoswitch, while specific binding is completely switched off in the other state. With regard to the second goal, accompanying molecular dynamics simulations combined with a quantitative structure activity relationship revealed that the alpha-helicity of the S-peptide in the binding pocket correlates surprisingly well with measured dissociation constants. Moreover, the simulations show that both configurations of all S-peptides exhibit quite well-defined structures, even in apparently disordered states.

DOI: https://doi.org/10.1021/jacs.9b03222

Photocontrolling Protein-Peptide Interactions: From Minimal Perturbation to Complete Unbinding

Brankica Jankovic,[1,3] Adnan Gulzar[2,3], Claudio Zanobini,[1]
Olga Bozovic,[1] Steffen Wolf[2], Gerhard Stock,[2,4] Peter Hamm[1,4]
[1] *Department of Chemistry, University of Zurich, Zurich, Switzerland*
[2] *Biomolecular Dynamics, Institute of Physics, Albert Ludwigs University, Freiburg, Germany*
[3] *both authors contributed equally*
[4] *corresponding authors:* peter.hamm@chem.uzh.ch and stock@physik.uni-freiburg.de
(Dated: May 16, 2019)

Abstract: An azobenzene-derived photoswitch has been covalently cross-linked to two sites of the S-peptide in the RNase S complex in a manner that the α-helical content of the S-peptide reduces upon *cis*-to-*trans* isomerization of the photoswitch. Three complementary experimental techniques have been employed, isothermal titration calorimetry (ITC), circular dichroism (CD) spectroscopy and intrinsic tyrosine fluorescence quenching, to determine the binding affinity of the S-peptide to the S-protein in the two states of the photoswitch. Five mutants with the photoswitch attached to different sites of the S-peptide have been explored, with the goal to maximize the change in binding affinity upon photoswitching, and to identify the mechanisms that determine the binding affinity. With regard to the first goal, one mutant has been identified, which binds with reasonable affinity in the one state of the photoswitch, while specific binding is completely switched off in the other state. With regard to the second goal, accompanying molecular dynamics (MD) simulations combined with a quantitative structure activity relationship (QSAR) revealed that the α-helicity of the S-peptide in the binding pocket correlates surprisingly well with measured dissociation constants. Moreover, the simulations show that both configurations of all S-peptides exhibit quite well-defined structures.

I. INTRODUCTION

Understanding conformational and dynamic aspects of protein-protein interactions is of paramount importance for new strategies in controlling them. In order to employ time-resolved techniques for the investigation of conformational changes of proteins and/or peptides, e.g., by transient X-ray scattering[1] or transient IR spectroscopy,[2] fast triggering of a given process is required. This is where the importance for external control of specific interactions emerges - it facilitates detailed understanding of real-time conformational changes induced by protein-peptide recognition. Photocontrol has been recognized as a valuable tool for the external manipulation of numerous *in vitro* as well as *in vivo* processes. This way of triggering conformational changes offers numerous advantages, in particular high spatial and temporal resolution and selectivity.[3] Photoswitching, as one of the most promising approaches of photocontrol, has the additional advantage of being reversible.[4] For example, a reversible photocontrol of the α-helical content of small peptides with sufficient α-helical propensity can be achieved by crosslinking to sites of the peptide with an azobenzene-based molecule.[5–8] Upon illumination, the azobenzene chromophore undergoes a reversible *cis* to *trans* isomerization around its central diazene (N=N) double bond. Isomerization changes the geometry of the azobenzene moiety with different end-to-end distances of the two configurations, leading to either a perturbation or a stabilization of the helix, depending on the distance between sites to which the azobenzene moiety is bound.[9] Besides triggering folding/unfolding of small α-helices, azobenzene derivatives have also been incorporated in small cyclic peptides[10,11] and β-hairpins.[12–15] More complex structural processes induced by that concept include the folding/unfolding transition of relatively large proteins,[16,17] the modulation of enzymatic activity,[18–20] cell-cell adhesion,[21] or ion-channel activity.[3] *In vivo* applications became possible with the design of biocompatible azobenzene derivatives, e.g. in zebrafish embrios[22,23] or to control mitosis.[24]

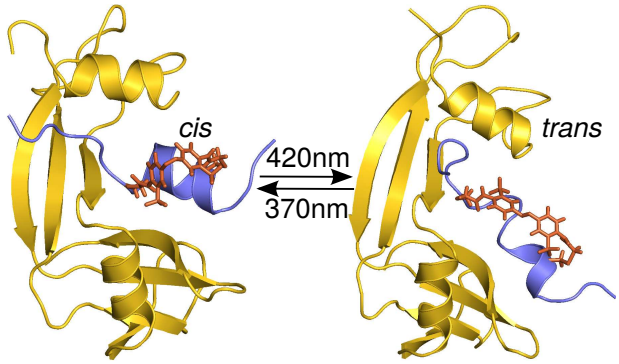

FIG. 1. Molecular construct studied in this work: S-protein (yellow) with S-pep(6,13) (blue) bound to it in the two states of the photoswitch (red).

In this study, we modulate the binding affinity within the non-covalent ribonuclease S complex (RNase S) with the ultimate goal of achieving photoinduced peptide unbinding. RNase S results from limited, site-specific hydrolysis of ribonuclease A, an enzyme from bovine pancreas.[25] Under controlled conditions, subtilisin can cleave a single peptide bond in RNase A and yields the

RNase S complex composed of the S-peptide (residues 1-20) and the S-protein (residues 21-124).[25] Full enzymatic activity is restored when the two components form a native-like complex. The three-dimensional structure of the complex is essentially the same as that of intact RNase A, except from small differences near the cleaved peptide bond.[26] Consequently, the S-peptide adopts an α-helical structure when it is bound to the S-protein, while it is essentially disordered when isolated in solution due to its short sequence.[27] This property makes RNase S an excellent model to study the question whether the recognition mechanism between the S-protein and S-peptide can be characterized as "induced-fit" or as "conformational selection".[28–31] Furthermore, it opens the possibility to phototrigger binding/unbinding of the S-peptide, adopting the concept that has previously been used to control the α-helical content of isolated peptides via cross-linking two sites of the helix with an azobenzene moiety.[5–8] Fig. 1 shows the construct we designed for this work: a S-peptide (blue) is bound to a S-protein (yellow), the former of which being photoswitchable and designed in a way that the azobenzene-moiety (red) in its *trans*-configuration destabilizes the α-helical content of the S-peptide.

There have been attempts to photocontrol RNase S in the past, mainly with the focus on influencing the enzymatic activity. Pioneering studies have been performed by Lui et al.[32] as well as Hamachi et al.[33] They created different mutants with the non-natural amino acid phenylazophenylalanine placed at different positions of the S-peptide. In contrast to our construct, the photoswitch does not cross-link two sites. Nonetheless, by photoswitching the configuration of the side chain, particularly at position 13 of the S-peptide,[33] the enzymatic activity in one of the photoswitch states was reported to completely cease. In the subsequent study of Woolley's group,[34] the same model system has been studied more extensively. They could not reproduce the results from Ref. 33, rather they found only a two-fold difference in the activity between *cis* and *trans* states. In this study, binding affinities were also estimated, albeit indirectly via the enzymatic activity results. The largest modulation they found for the binding affinity in the *cis* vs the *trans* state was a factor 5. A different protein system, that however uses a very similar design idea as our present one, has been reported by Kneissl et al.,[35] who designed photocontrollable α-helical model peptides that bind to the Bcl-xl protein and are relevant for apoptosis. Up to 20-fold difference in binding affinity have been reported upon *trans* to *cis* isomerization of the photoswitch, but specific binding was preserved in both states with binding affinities in the nanomolar range.

II. DESIGN CRITERIA

For the design of the photoswitchable S-peptides, the following basic criteria were considered:

- A water-soluble derivative of azobenzene has been used as photoswitch, BSBCA (3,3'-bis(sulfonato)-4,4'-bis(chloroacetamido) azobenzene).[36]
- A pair of amino acid residues needs to be replaced by cysteines for the site-selective linking of BSBCA. When choosing these sites, their effect for binding to the S-protein and/or the stability of the α-helix needs to be considered.
- Steric hindrance between crosslinked photoswitch and S-protein binding cleft should be avoided so that specific binding is preserved. To that end, the PyMOL software package[37] was used for visual examination and discrimination between solvent-exposed and non-solvent exposed amino acid residues of the S-peptide.
- The goal has been to stabilize the α-helical conformation in the more compact *cis* state of BSBCA, and to destabilize it in the *trans* state. This criterion determines the distance between sites that are being crosslinked.[9] To that end, we assumed an ideal length of BSBCA in its *cis* state of 11-16 Å,[17] and determined distances from the X-ray structure of RNase A (PDB code: 2E3W).[38]

Within that framework, five different photoswitchable S-peptide variants have been designed. Ala6 has been chosen as the first anchoring point in all but one S-peptide variants, since it is the first amino acid residue (starting from N-terminus) that is part of the α-helical region and at the same time is solvent-exposed in the complex. Furthermore, it has been shown to have no effect on the binding affinity or the structure of the RNase S complex.[28,31,39]

To obtain a prototype S-peptide that preserves binding, we started with Ser15 as second anchoring point, which also is known to be a residue that does not affect the binding,[28] and furthermore, it fulfills all aforementioned steric criteria; in particular, the end-to-end distance of the photoswitch in the *cis*-state fits the distance in the X-ray structure the best. We will denote that variant as S-pep(6,15). However, we learned quickly that this particular variant does not modulate the binding affinity significantly upon photoswitching, and we moved towards the next S-peptide variant, investigating the effect of a mutation that destabilizes the S-protein/S-peptide complex. We selected His12 for this purpose, whose mutation to Phe12 decreases the binding affinity by about a factor 25;[29] we will call that variant S-pep(6,15)H12F.

Furthermore, assuming that the α-helical content determines the binding, we considered S-pep(6,13) and S-pep(6,10) with shorter spacings 7 and 4, respectively, between the anchoring groups. According to Ref. 9, these spacings maximize the difference in stability of an α-helix with the photoswitch in the *cis* vs the *trans* states. Finally, we explored one variant in which we varied the starting point by one amino acid, S-pep(7,11), again with spacing 4. The amino acids that are affected in this case,

Lys7 and Gln11, were both shown to play a role in the stabilization of the helix and in complex formation.[40,41]

III. MATERIALS AND METHODS

A. Preparation and Purification of S-Protein and S-Peptide Variants

The S-protein was prepared from the commercial bovine ribonuclease A (Sigma Aldrich) by limited proteolysis with subtilisin, in essence as described in Refs. 25 and 42. The proteolysis mixture was then applied to size-exclusion chromatography on Sephadex G-75 in order to isolate the S-protein from the S-peptide as well as from subtilisin and residual unhydrolized RNase A. Wild-type S-peptide (sequence KETAAAK-FERQHMDSSTSAA) and four modified S-peptide mutants with pairs of cysteine residues on different positions (i.e., S-pep(6,15), S-pep(6,13), S-pep(6,10) and S-pep(7,11), see Sec. II) were synthesized by standard fluorenylmethoxycarbonyl(Fmoc)-based solid-phase peptide-synthesis on a Liberty 1 peptide synthesizer (CEM Corporation, Matthews, NC, USA). For S-pep(6,15)H12F, an additional His-to-Phe mutation was introduced at position 12. All amino acids were purchased from Novabiochem (La Jolla, CA, USA). The peptides were subsequently purified using reverse-phase C18 HPLC chromatography with an acetonitrile gradient 0-100% in 10 column volumes. The cysteine residues were subsequently cross-linked with the photoisomerizable linker BSBCA,[36] and purified again with the same conditions as in the previous step. The purity of S-protein and all S-peptide variants was confirmed by mass-spectrometry. Solutions of S-protein and S-peptide variants were prepared in 50 mM sodium phosphate buffer at pH 7.0. Concentrations have been determined by amino acid analysis.

The *trans*-configuration is the thermodynamically more stable one and accumulates to essentially 100% upon thermal relaxation, which happens on a timescale of 1-10 h (see Supporting Information, Fig. S1A). Typically, we left the sample in dark overnight before an experiment of the *trans*-configuration was performed. To prepare the *cis*-configuration, we illuminated the sample with a 370 nm cw diode laser (90 mW, CrystaLaser). Its power is sufficient to switch a sample in minutes, and we verified that >85% *cis* are prepared in that way (see Fig. S1B and its discussion).

B. Isothermal Titration Calorimetry

The isothermal titration calorimetry (ITC) measurements were performed on a MicroCal iTC200 from Malvern (Malvern, UK) at 25°C or 21°C for wild-type and photoswitchable S-peptides, respectively. The sample cell contained 250 μL of S-protein solution at concentrations that varied according to the expected affinity. 10x higher S-peptide concentration was titrated into the sample cell. The first injection was 0.4 μL and subsequent injections every 120 s were 2.0 μL. We verified that ITC reveals reliable results for the binding affinity also in the *cis*-state, despite the fact that the overall measurement time is comparable to that of the thermal *cis*-to-*trans* back-isomerization for the free peptide, and despite the fact that this reaction releases heat[43] that is comparable to the heat of binding (see Fig. S1A and its discussion). K_d's were determined from the ITC data using the instrument's software and assuming one binding site.

C. CD Measurements

Circular Dichroism (CD) measurements were performed on a Jasco (Easton, MD) model J-810 spectropolarimeter in a 0.1 cm quartz cuvette. We made sure the measurement was fast enough to prevent significant amount of thermal back-isomerization, and that the intensity of the light used by the CD spectrometer was low enough so the amount of molecules that photoisomerized due to that light is negligible (see Fig. S2 in SI).

D. Intrinsic Tyrosine Fluorescence Quenching

Fluorescence measurements were performed using two different fluorimeters. A commercial instrument (PerkinElmer) was used for the wild-type S-peptide, setting excitation and emission wavelengths to 285 nm and 306 nm, respectively. A larger sensitivity was needed for the photoswitchable variants due to the large absorption of the photoswitch itself, which furthermore changes between *cis* and *trans* states, and hence required extremely low concentration to avoid fluorescence re-absorption (optical densities were kept below OD=0.05). At the same time, the excitation intensity needed to be very low to avoid inducing isomerization of the photoswitch during the course of the measurement (see SI for details). The larger sensitivity was achieved with a home-built fluorimeter, that employed 266 nm for the excitation obtained from the 3rd harmonic of a Ti:Sapphire amplified laser system (Spectra Physics, Spitfire). The fluorescence was detected in a 90 degrees geometry using a single photon counter (PMA 175-N-M, PicoQuant) together with a special filter (XRR0340 Asahi Spectra USA) to remove both the 266 nm and the 370 nm radiations needed to promote the fluorescence of the tyrosine's and the *trans* to *cis* isomerization of the photoswitch, respectively.

E. MD Simulations

To generate initial structures of RNase S for the MD simulations, we started with the RNase complex struc-

ture (PDB ID 1Z3P),[44] mutated Nva13 to Met13, and then attached five additional residues from an X-ray structure of RNase A (PDB ID 2E3W)[38] at the C-terminus of the S-peptide. Following the procedure from Ref. 45, we next attached the azobenzene photoswitch on cysteine side chains by mutating the respective residues i, j of S-peptides according to experimental labeling positions (see Sec. II). All MD simulations were performed using the GROMACS software package v4.6.7 (Ref. 46) with hybrid GPU-CPU acceleration scheme, the Amber03ws forcefield[47] and TIP4P-2005 water[48] solvent molecules. After energy minimization, all systems were equilibrated for 10 ns, and simulated at 300 K for at least 400 ns (see Supporting Information for details). Moreover, a MD simulation of wild type RNase S was performed, in order to show the similarity of the conformational distributions of crosslinked vs native peptides (Fig. S3).

MD trajectories were preprocessed by performing a principal component analysis on backbone dihedral angles (dPCA+)[49] of residues 3 to 13 of S-peptides. Including only the first few principal components with 80% of the total sum of eigenvalues (depending on the individual system, about five to six), we define a reduced coordinate space of significantly lower dimensionality.[50] After dimensionality reduction, robust density-based clustering[51] was performed to identify the metastable conformational states of the individual systems (see Supporting Information for details). On the basis of most populated states, representative structures and respective flexibilities were obtained by employing *gmx rmsf* and displayed via *PyMOL*.[37]

IV. RESULTS

We used three independent methods to determine the binding affinity of the various S-peptides to the S-protein, isothermal titration calorimetry (ITC), circular dichroism (CD) spectroscopy and intrinsic tyrosine fluorescence quenching. Each one of these methods focuses on different aspects of binding, and has its strengths and weaknesses. For some of the S-peptides, more than one method could be applied with reasonable confidence, allowing us to cross-validate the results.

Starting with the "gold standard", ITC,[52] it was possible to determine binding affinities for relatively strong binders, see Fig. 2 and Tab. I. Due to the limited solubility of both the S-protein and the S-peptide, we could not determine the binding affinity of S-pep(6,13) in either state of the photoswitch, and, more severely, also not for the *trans*-configuration of most of the other S-peptides, with the one exception of S-pep(6,15), for which the effect of switching is negligible.

We therefore turn to CD spectroscopy in the next step, as our starting assumption has been that the photoswitch in the *trans*-configuration perturbs the helical conformation of the S-peptide, and CD spectroscopy is sensitive

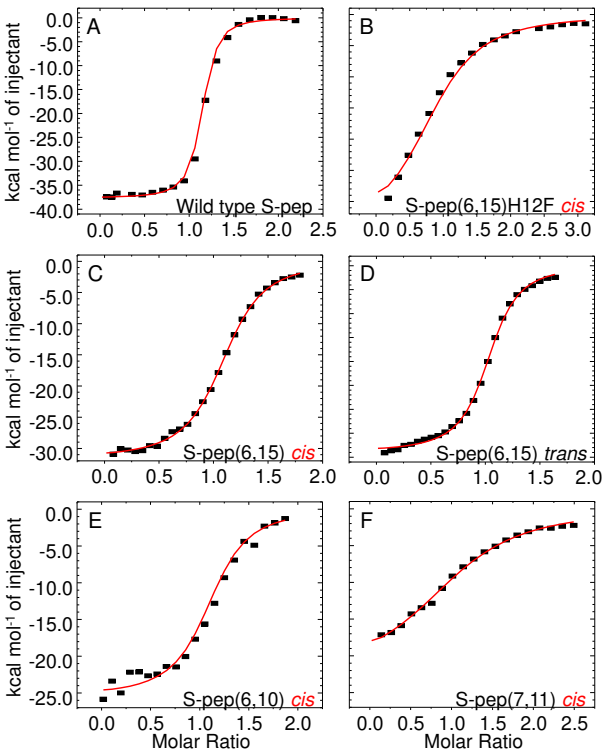

FIG. 2. ITC thermograms of the S-protein and different S-peptide variants. (A) Wild-type S-peptide, (B) S-pep(6,15)H12F-*cis*, (C) S-pep(6,15)-*cis*, (D) S-pep(6,15)-*trans*, (E) S-pep(6,10)-*cis* and (F) S-pep(7,11)-*cis*.

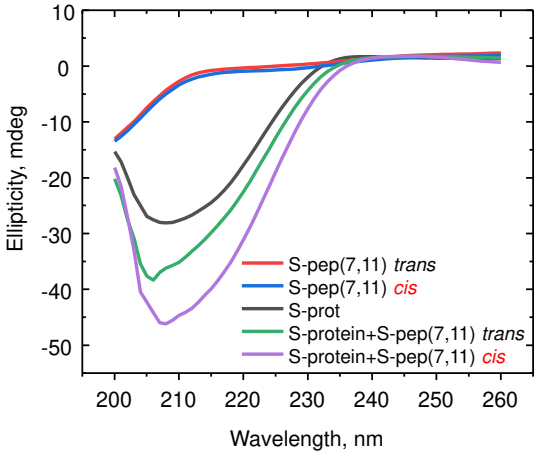

FIG. 3. CD spectra of the S-peptide alone in *trans* (red) and *cis* (blue), the S-protein alone (black), and the S-protein with S-peptide in the *trans* (green) and *cis* state (purple), exemplified here for S-pep(7,11).

to exactly that structural aspect. To set the stage, we show in Fig. 3 CD spectra of the S-pep(7,11) alone in its two states (red and blue), of the S-protein alone (black), as well as of mixtures of both at a concentration where the amount of binding has been ≈25% in the *trans*-state, and ≈75% in the *cis*-state (*vide infra*). For the S-peptide

TABLE I. Dissociation constants K_d (in μM) of the various S-peptide variants and the S-protein, as determined by ITC, CD and intrinsic tyrosine fluorescence quenching.

	ITC		CD		fluorescence	
	cis	*trans*	*cis*	*trans*	*cis*	*trans*
S-pep(6,15)	1.5±0.2	1.2±0.8	1.7±1.0	2.9±0.8	3.6±0.9	3.2±1.3
S-pep(6,15)H12F	1.9±0.4	-	1.5±0.5	21±1.8	-	-
S-pep(6,13)	-	-	70±20	*[a]	130±30	*[b]
S-pep(6,10)	0.6±0.2	-	2.3±1.2	47±10	-	-
S-pep(7,11)	5.9±0.2	-	6.2±2.9	125±15	-	-
wild type	0.11±0.01		0.14±0.04		0.14±0.02	

[a] no binding was observed

[b] unspecific binding was observed, however, since the saturation plateau could not be reached, the binding constant could not be determined.

alone, the CD spectra indicate a predominantly random-coil conformation, regardless of the state of the photoswitch (see Fig. 3, red and blue). This finding is in agreement with the well-known fact that the S-peptide is disordered when it is free in solution.[29] The structural constrain of the photoswitch does not lead to any significant stabilization of the helical structure in the isolated form. Once bound to S-protein, however, the S-peptide adopts a helical structure, as deduced from a CD signal (Fig. 3, green and purple) that is significantly larger than the sum of the signals from the S-peptide alone (red and blue) and S-protein alone (black). Furthermore, the results show that there are significant differences in helical content between the *cis* and *trans* states, indicating a larger amount of binding due to a higher affinity in the *cis*-state.

Besides folding of the S-peptide upon binding, the contribution of the S-protein *per se* to the overall CD signal might change as well. That can be seen from the fact that the difference between e.g. the purple line in Fig. 3 (S-protein plus ≈75% of bound S-pep(7,11)-*cis*) and the black line (S-protein alone) is much bigger than what the size of the fragments would suggest (20 amino acids for the S-peptide vs 104 amino acids of the S-protein). Indeed, it has been suggested that the S-protein is much more flexible in the absence of the S-peptide,[53] which is also the reason for difficulties in obtaining a crystal structure. Along these lines, a recent MD simulation has shown that helix II of the S-protein unfolds when the S-peptide unbinds.[31]

To determine the binding affinity, the CD signal at 225 nm[54] was measured as a function of S-peptide concentration, keeping the concentration of the S-protein constant at around 50 μM, see Fig. 4. In these plots, "0%-fraction-bound" corresponds to the CD signal calculated as a trivial sum of the contributions from S-peptide alone and S-protein alone, and "100%-fraction-bound" to the plateau value reached at high enough S-peptide concentrations. To determine the binding affinity K_d, the data were fit to a chemical equilibrium, $P + L \rightleftharpoons PL$. Tab. I summarizes the results. It turns out that the method is more reliable for weak binders and as such complementary to ITC. That is, if the binding affinity becomes too large with K_d's much smaller than the concentration of the S-protein, the binding curve adopts a kink-like behaviour (see in particular the wild-type data in Fig. 4A) and the fit parameters become very insensitive to K_d; in

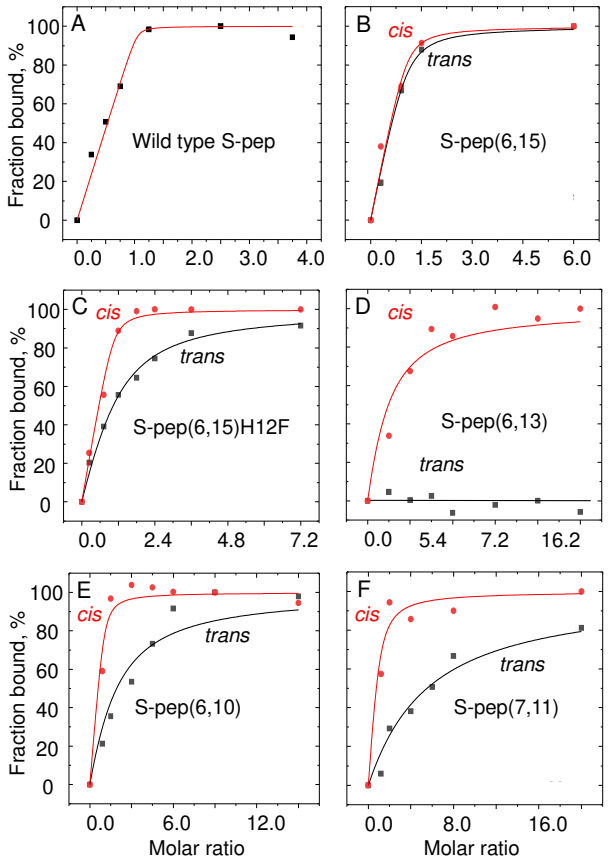

FIG. 4. CD binding curves for various S-peptide variants. (A) Wild type, (B) S-pep(6,15) (C) S-pep(6,15)H12F, (D) S-pep(6,13), (E) S-pep(6,10), and (F) S-pep(7,11). Measurements with the photoswitch in *cis* configuration are plotted in red, those in the *trans* configuration in black.

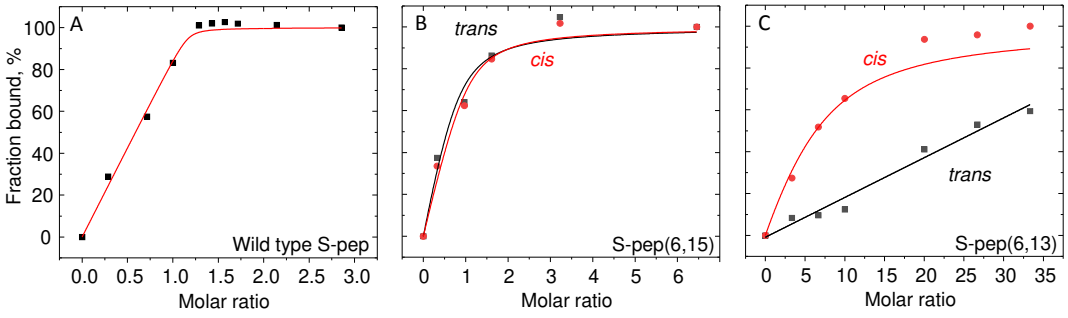

FIG. 5. Fluorescence binding curves for various S-peptide variants. (A) Wild type, (B) S-pep(6,15), and (C) S-pep(6,13). Measurements with the photoswitch in *cis* configuration are plotted in red, those in the *trans* configuration in black. In the case of S-pep(6,13)-*trans*, the saturation plateau was not reached; it was assumed to be the same as for S-pep(6,13)-*cis* for the purpose of plotting (but that does not have to be correct since unspecific binding implies that more than one S-peptide might bind). The linear fit in this case is to guide the eyes.

essence it is then a single data point at the kink that determines K_d. Fortunately, both ITC and CD works reasonably well for S-pep(6,15), allowing us to cross-validate the two methods.

Finally, fluorescence quenching was employed as method to determine the binding dissociation constants for the *cis* and the *trans* forms of some of the peptides. The intrinsic tyrosine S-protein fluorescence decreases by circa 20% upon binding in all cases. Local structural aspects like changes of the chemical environment via hydrogen bonds, disulfide bridges formation/breaking and resonance energy transfer mechanism can affect the intrinsic tyrosine fluorescence quenching of RNase S.[55,56] The obtained binding curves are shown in Fig. 5, where the values for "0%-fractional-bound" and "100%-fraction-bound" have been determined in the same way as for the CD data. Wild type and S-pep(6,15) were used to cross-validate the fluorescence method with CD and ITC techniques, with both the commercial and the home-built fluorimeters, respectively, and S-pep(6,13) was then measured as an example with very low binding affinity. The extracted binding affinities are summarized in Tab. I. Overall, the results from three different methods are in good agreement with each other within experimental error.

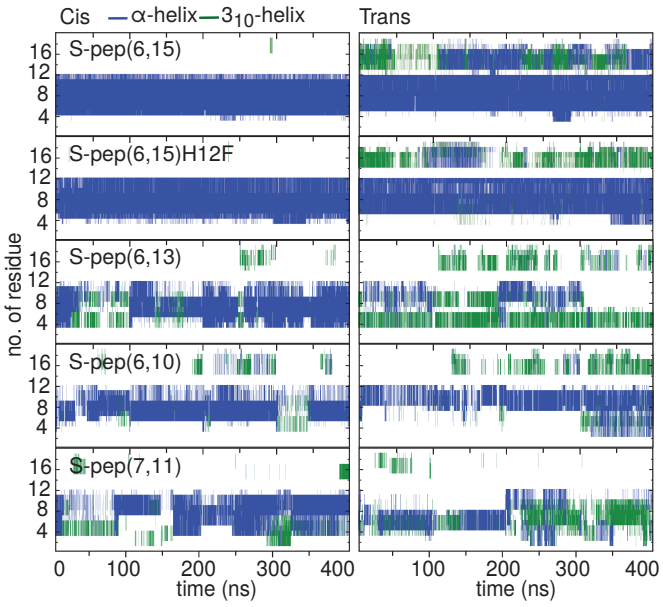

FIG. 6. Time evolution of the S-peptides' secondary structure in *cis* (left) and *trans* (right) configuration, obtained from all-atom MD simulations after suitable equilibration (see Methods). α helix content in blue, 3_{10} helix in green, unstructured parts in white.

A. Computational Results

To study the relation between changes in binding affinity (i.e, experimental K_d obtained by CD spectroscopy) and secondary structural changes of the S-peptides, all-atom MD simulations were performed as described in Methods. As an overview, Fig. 6 shows the resulting dynamics of secondary structures of the various S-peptides obtained from DSSP analysis.[57,58] In particular, we focus on the differences of helicity when changing from *cis* to *trans* configuration. In the case of S-pep(6,15) and S-pep(6,15)H12F, we find that the core region formed by residues 4-11 exhibits a stable α-helical conformation in both *cis*- and *trans*-configuration. Recalling that an α-helix of residues Thr3-Met13 is the hallmark of the native, active RNase S,[29] we conclude that the structure of these S-peptides are hardly perturbed by the photoswitch. This conclusion is also supported by the fact that the wild-type peptide exhibits about the same helicity as S-pep(6,15) and S-pep(6,15)H12F (see Fig. S3). S-pep(6,13), on the other hand, is significantly more affected by *cis* $\rightarrow$ *trans* photoswitching. Apart from infrequent short perturbations, S-pep(6,13)-*cis* reveals a relatively stable α-helical structure, while its *trans* form

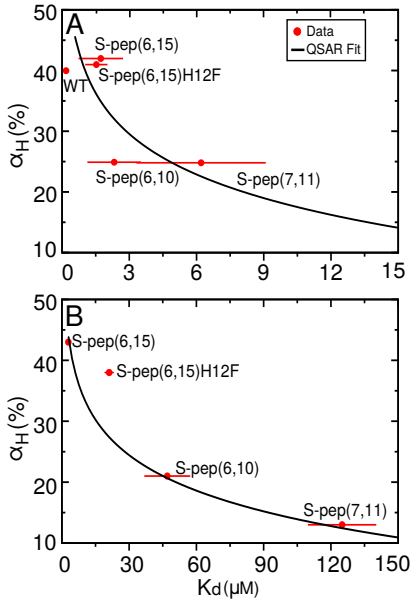

FIG. 7. (A) α-helicity vs experimental K_d in *cis*-configuration, together with the wild-type (WT), and fit obtained by Eq. 1. (B) The same for the *trans*-configuration.

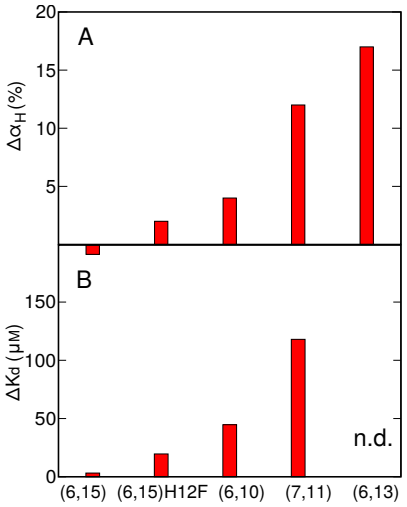

FIG. 8. (A) change in α-helicity difference: $\Delta\alpha_H = \alpha_{H(cis)} - \alpha_{H(trans)}$ and (B) change in experimental $\Delta K_d = K_{d(trans)} - K_{d(cis)}$, as determined from CD spectroscopy (Table I). No experimental exist for K_d in the *trans*-state of S-pep(6,13), which is why no bar is shown in panel (B), but it is clear from Figs. 4D and 5C that the difference is large.

mostly exist as a 3_{10} helix or random coil. In a similar way, S-pep(6,10) and S-pep(7,11) exhibit decreased α-helicity upon *cis* $\rightarrow$ *trans* photoswitching, although the structural changes found in *trans* are less prominent compared to S-pep(6,13). Performing a time average over the trajectories, the above findings can be represented by a probability distribution of the α-helicity of the various systems (see Fig. S3, Supporting Information).

To connect these computational results for the α-helicity α_H to the experimental findings of K_d in form of a quantitative structure activity relationship (QSAR), we used a Boltzmann statistics-based ansatz, which assumes that the free energy of binding, $\Delta G \sim \ln(K_d)$, is linearly dependent on the number of peptide residues in α-helical conformation. This gives

$$\alpha_H = -c_\alpha k_B T \ln(K_d) + \alpha_{H_0}, \qquad (1)$$

where c_α accounts for the free energy gain per helical residue $\Delta G = \alpha_H/c_\alpha$, and α_{H_0} is a reference peptide helicity. As shown in Figure 7, this ansatz reveals a convincing fit ($R^2 = 0.85$) for the *trans*-state. The fit is less clear ($R^2 = 0.65$) for the *cis*-state, where we also added the results of the wild-type. The resulting fit parameters for *trans* ($c_\alpha = 3.4 \pm 0.9$, $\alpha_{H0} = 53 \pm 6$) and *cis* ($c_\alpha = 4.2 \pm 2.5$, $\alpha_{H0} = 44 \pm 6$) agree with each other within their error ranges.

Figure 8 combines these results and correlates the change of the calculated change in α-helicity $\Delta\alpha_H = \alpha_{H(cis)} - \alpha_{H(trans)}$ to the experimentally measured change in affinity $\Delta K_d = K_{d(trans)} - K_{d(cis)}$. In nice agreement, both simulated $\Delta\alpha_H$ and experimental ΔK_d show an ascending behaviour starting with S-pep(6,15) via S-pep(6,15)H12F and S-pep(6,10) to S-pep(7,11) and S-pep(6,13).

It is interesting to connect the above discussed helicity changes with the prevailing molecular structures of the S-peptides. To this end, robust density-based clustering[51] (see Methods) was performed for all systems and the resulting main conformational states were analyzed in detail (see Figs. S4 and S5, Supporting Information). Overall, we find that all S-peptides can be well described by only four conformational states, where the dominant state typically occurs with 40-70% population. Figure 9 shows the resulting main structure of all S-peptides (the S-protein is not shown for clarity). In line with the discussion of Fig. 6, we find that *cis* $\rightarrow$ *trans* photoswitching has the least impact on the secondary structures of S-pep(6,15) and S-pep(6,15)H12F, while the most significant changes are found for S-pep(6,13), which essentially loses its α-helical conformation. Coloring residues according to their fluctuations, we find that the structures are well defined in both *cis* and *trans* and exhibit increased flexibility only at the terminals. That is, even the apparently disordered regions of S-pep(6,13) and S-pep(7,11) reveal stable structures.

V. DISCUSSION AND CONCLUSION

To facilitate photocontrolling of peptide-protein binding, we have designed various photoswitchable S-peptides, switching their helical content, and measured their binding affinities to the S-protein using a variety of experimental techniques (Table I). Alpha helices are structural motifs that very commonly are relevant

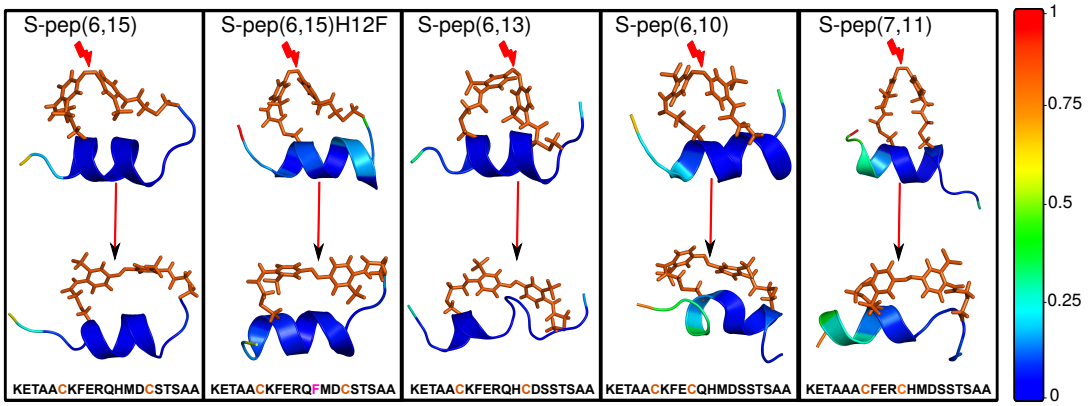

FIG. 9. Most populated structures obtained from a clustering analysis, see text and Supporting Information for details. The S-protein is not shown for clarity. The residues are colored according to normalized root mean square fluctuations.

for protein-protein, protein-peptide and protein-DNA interactions and therefore represent important targets for modulation of binding affinities. Here, we have introduced a concept by which the helical content can be modulated in a very controlled manner. The overall disruption of secondary structures not only depends upon the distance between anchor residues of photoswitch but also on the exact position of the photoswitch.

By performing MD simulations of the *cis* and *trans* configurations of the RNase S complex, we were able to relate simulated α-helicities α_H to experimentally obtained binding affinities K_d, which are in surprisingly good agreement (Fig. 8). Using the simple QSAR ansatz of Eq. 1, we have shown that the α-helicity is inversely related to the experimental K_d's (Figs. 7). This suggests that relatively short (sub-μs) MD simulations are indicative of the long-time binding or dissociation behavior of the RNase S complex. The secondary structure analysis of the S-peptides in (Fig. 9) shows a significant decrease in α-helicity upon *cis*-to-*trans* isomerization for all systems, with the one exception of S-pep(6,15). The latter is in line with the findings of Ref. 9 studying the photoswitching of isolated helical peptides, which revealed that the (i,i+9) spacing in S-pep(6,15) is the dividing point between decreasing or increasing the α-helical content upon *cis*-to-*trans* isomerization.

The largest change in α-helicity is found for S-pep(6,13) and S-pep(7,11) with spacings (i,i+7) and (i,i+4), respectively. The corresponding structures of the *trans* forms in Fig. 9 reveal a considerable loss of α-helical conformation. In particular, S-pep(6,13)-*trans* adopts a helical conformation only at its N-terminal, while its C-terminus is completely disordered. It has been suggested that the N-terminal part of the S-peptide is unzipping from the S-protein binding groove due to equilibrium state fluctuations.[31] Furthermore, based on an alanine mutant screening approach,[31] it has been shown that the N-terminus (more precisely residues 1-7) contributes to binding only to a minor extent. Hence, even though a small percentage of helicity was preserved in the case of S-pep(6,13)-*trans*, no specific binding is observed, since the residual helicity is located in relatively unimportant part for the binding.

It is interesting to note that the isomerization of the photoswitch does not lead to a significant increase of peptide fluctuations. Instead, Figs. 9 and S4 (see Supporting Information) suggest that peptide structures are mostly well defined in both the *cis* and the *trans*-state and exhibit fluctuations only at the termini. Especially the parts of the peptide that lie between the clamping points of the photoswitch display highly stable structures, even in apparently disordered states. Furthermore, in the case of S-pep(6,13), the peptide structure is more stable in the disordered *trans* state than in helical *cis* state, in clear contrast to intuition. This stabilization of disordered states turns out to be one of the most interesting outcomes of our photolabeling strategy. In combination with structural predictions from MD simulations, it allows a rather distinct manipulation of the peptide structure depending on the photoswitch attachment points.

We consider S-pep(6,13) the most interesting result in our series of mutants. Firstly, while no binding could be detected for S-pep(6,13)-*trans* via CD spectroscopy (Fig. 4D), some degree of binding is observed by fluorescence quenching (Fig. 5C), illustrating the different aspects of binding the two methods are sensitive to. That is, while CD measures helical content, fluorescence quenching measures spatial proximity. The difference between CD and fluorescence data can probably be explained by the fact that binding is unspecific in this case, i.e., more in the sense of aggregation, and hence does not induce any α-helical structure. Since we did not reach a plateau in fluorescence intensity in this case, we cannot truly quantify the binding affinity, but it is probably in the mM range. And indeed, such weak binding can typically no longer be characterized as "specific", in particular if the binding partner is a floppy peptide like in the present case.[59]

Secondly, the largest effects observed in literature for photoswitchable protein-peptide complexes are K_d ratios

of about 20 (Ref. 35), and the effect is equally large for S-pep(6,10) and S-pep(7,11). For S-pep(6,13), the ratio is even larger, i.e., effectively infinite, as no specific binding is detectable by CD spectroscopy in the *trans*-state. To the very best of our knowledge, such a big effect has not been achieved so far for any photoswitchable protein-peptide complex. This property makes the system particularly interesting for time-resolved studies, in which the light-driven isomerization of the photoswitch triggers unbinding of the S-peptide, and the structural response of the protein is investigated by e.g. transient IR spectroscopy or transient X-ray scattering experiments in upcoming free electron lasers.[1] Ideally, in such an experiment, the S-peptide should unbind as quickly as possible; only then the temporal ordering of unbinding event vs structural response could be measured, addressing the long-standing question whether the process can be described as "conformational selection" or as "induced fit". However, the unbinding rate constant k_{off} scales essentially as K_d (since k_{on} is limited by diffusion and as such essentially a constant), hence to speed up k_{off}, K_d in one state of the photoswitch should be as large as possible. Transient IR experiments are currently underway.

Supporting Information: Experimental validation of ITC as a method to determine binding affinities also in the *cis*-state (Fig. S1A and its discussion), the amount of *cis* prepared by illumination at 370 nm (Fig. S1B and its discussion), the effect of the measurement light in CD and fluorescence spectroscopy (Fig. S2 and its discussion), more detailed MD methods, description of the helicity and contacts of wild type and labeled systems (Fig. S3), as well as detailed results of the clustering analysis (Figs. S4 and S5) can be found in Supporting Information. This information is available free of charge on the ACS Publications website.

Acknowledgement: We thank Ilian Jelezarov for important discussions concerning the ITC, Rolf Pfister for the synthesis of the peptides and BSBCA, Ben Schuler and his group for their continuous help with the protein chemistry, and the Functional Genomics Center Zurich, especially Serge Chesnov for help with the mass spectrometry and Birgit Roth for amino acid analysis. The work has been supported in part by the Swiss National Science Foundation (SNF) through Grant 200021_165789, as well as by the Deutsche Forschungsgemeinschaft through Grant STO 247/10-2. We acknowledge support by the High Performance and Cloud Computing Group at the Zentrum für Datenverarbeitung of the University of Tübingen, the state of Baden-Württemberg through bwHPC and the German Research Foundation (DFG) through grant no INST 37/935-1 FUGG (RV bw16I016) and the Black Forest Grid Initiative.

References:

(1) Standfuss, J. Membrane protein dynamics studied by X-ray lasers – or why only time will tell, *Curr. Opin. Struct. Biol.* **2019**, *57*, 63–71.

(2) Hamm, P.; Helbing, J.; Bredenbeck, J. Two-Dimensional Infrared Spectroscopy of Photoswitchable Peptides, *Annu. Rev. Phys. Chem.* **2008**, *59*, 291–317.

(3) Zatsepin, T. S.; Abrosimova, L. A.; Monakhova, M. V.; Le Thi Hien.; Pingoud, A.; Kubareva, E. A.; Oretskaya, T. S. Design of photocontrolled biomolecules based on azobenzene derivatives, *Russ. Chem. Rev.* **2013**, *82*, 942–963.

(4) Beharry, A. A.; Woolley, G. A. Azobenzene photoswitches for biomolecules, *Chem. Soc. Rev.* **2011**, *40*, 4422–4437.

(5) Kumita, J. R.; Smart, O. S.; Woolley, G. A. Photocontrol of helix content in a short peptide, *Proc. Natl. Acd. Sci. USA* **2000**, *97*, 3803–3808.

(6) Bredenbeck, J.; Helbing, J.; Kumita, J. R.; Woolley, G. A.; Hamm, P. alpha-Helix formation in a photoswitchable peptide tracked from picoseconds to microseconds by time resolved IR spectroscopy, *Proc. Natl. Acad. Sci. USA* **2005**, *102*, 2379–2384.

(7) Woolley, G. A. Photocontrolling peptide alpha helices, *Acc. Chem. Res.* **2005**, *38*, 486–493.

(8) Ihalainen, J. A.; Paoli, B.; Muff, S.; Backus, E. H. G.; Bredenbeck, J.; Woolley, G. A.; Caflisch, A.; Hamm, P. Alpha-Helix folding in the presence of structural constraints., *Proc. Natl. Acad. Sci. USA* **2008**, *105*, 9588–9593.

(9) Flint, D. G.; Kumita, J. R.; Smart, O. S.; Woolley, G. A. Using an Azobenzene Cross-Linker to Either Increase or Decrease Peptide Helix Content upon Trans-to-Cis Photoisomerization, *Chem. Biol.* **2002**, *9*, 391–397.

(10) Bredenbeck, J.; Helbing, J.; Sieg, A.; Schrader, T.; Zinth, W.; Renner, C.; Behrendt, R.; Moroder, L.; Wachtveitl, J.; Hamm, P. Picosecond conformational transition and equilibration of a cyclic peptide, *Proc. Natl. Acad. Sci. USA* **2003**, *100*, 6452–6457.

(11) Satzger, H.; Root, C.; Renner, C.; Behrendt, R.; Moroder, L.; Wachtveitl, J.; Zinth, W. Picosecond dynamics in water-soluble azobenzene-peptides., *Chem. Phys. Lett.* **2004**, *396*, 191–197.

(12) Aemissegger, A.; Krautler, V.; van Gunsteren, W. F.; Hilvert, D. A photoinducible beta-hairpin, *J. Am. Chem. Soc.* **2005**, *127*, 2929–2936.

(13) Jurt, S.; Aemissegger, A.; Güntert, P.; Zerbe, O.; Hilvert, D. A Photoswitchable Miniprotein Based on the Sequence of Avian Pancreatic Polypeptide, *Angew. Chem. Int. Ed.* **2006**, *45*, 6297–6300.

(14) Dong, S. L.; Loweneck, M.; Schrader, T. E.; Schreier, W. J.; Zinth, W.; Moroder, L.; Renner, C. A photocontrolled beta-hairpin peptide, *Chem. - A Eur. J.* **2006**, *12*, 1114–1120.

(15) Schrader, T. E.; Schreier, W. J.; Cordes, T.; Koller, F. O.; Babitzki, G.; Denschlag, R.; Renner, C.; Löweneck, M.; Dong, S.-L.; Moroder, L.; Tavan, P.; Zinth, W. Light-triggered beta-hairpin folding and unfolding, *Proc. Natl. Acad. Sci. USA* **2007**, *104*, 15729–15734.

(16) Lorenz, L.; Kusebauch, U.; Moroder, L.; Wachtveitl, J. Temperature- and Photocontrolled Unfolding/Folding of

a Triple-Helical Azobenzene-Stapled Collagen Peptide Monitored by Infrared Spectroscopy, *ChemPhysChem* **2016**, *17*, 1314–1320.
(17) Zhang, F.; Zarrine-Afsar, A.; Al-Abdul-Wahid, M. S.; Prosser, R. S.; Davidson, A. R.; Woolley, G. A. Structure-based approach to the photocontrol of protein folding, *J. Am. Chem. Soc.* **2009**, *131*, 2283–2289.
(18) Schierling, B.; Noel, A.-J.; Wende, W.; Hien, L. T.; Volkov, E.; Kubareva, E.; Oretskaya, T.; Kokkinidis, M.; Rompp, A.; Spengler, B.; Pingoud, A. Controlling the enzymatic activity of a restriction enzyme by light, *Proc. Natl. Acad. Sci. USA* **2010**, *107*, 1361–1366.
(19) Hoersch, D. Engineering a light-controlled F 1 ATPase using structure-based protein design , *PeerJ* **2016**, *4*, e2286.
(20) Eisel, B.; Hartrampf, F. W.; Meier, T.; Trauner, D. Reversible optical control of F1Fo-ATP synthase using photoswitchable inhibitors, *FEBS Lett.* **2018**, *592*, 343–355.
(21) Ritterson, R. S.; Kuchenbecker, K. M.; Michalik, M.; Kortemme, T. Design of a photoswitchable cadherin, *J. Am. Chem. Soc.* **2013**, *135*, 12516–12519.
(22) Beharry, A. A.; Wong, L.; Tropepe, V.; Woolley, G. A. Fluorescence imaging of azobenzene photoswitching in vivo, *Angew. Chemie - Int. Ed.* **2011**, *50*, 1325–1327.
(23) Wachtveitl, J.; Zumbusch, A. Azobenzene: An Optical Switch for in vivo Experiments, *ChemBioChem* **2011**, *12*, 1169–1170.
(24) Borowiak, M.; Nahaboo, W.; Reynders, M.; Nekolla, K.; Jalinot, P.; Hasserodt, J.; Rehberg, M.; Delattre, M.; Zahler, S.; Vollmar, A.; Trauner, D.; Thorn-Seshold, O. Photoswitchable Inhibitors of Microtubule Dynamics Optically Control Mitosis and Cell Death, *Cell* **2015**, *162*, 402–411.
(25) Richards, F. M.; Vithayathil, P. J. The Preparation of Subtilisin-modified Ribonuclease and the Separation of the Peptide and Protein Components, *J. Biol. Chem.* **1959**, *234*, 1459–1465.
(26) Wlodawer, A.; Sjolin, L. Hydrogen exchange in RNase A: Neutron diffraction study, *Proc. Natl Acad. Sci. USA* **1982**, *79*, 1418–1422.
(27) Schreier, A. A.; Baldwin, R. L. Mechanism of Dissociation of S-Peptide from Ribonuclease, *Biochemistry* **1976**, *16*, 4203–4209.
(28) Goldberg, J. M.; Baldwin, R. L. A specific transition state for S-peptide combining with folded S-protein and then refolding, *Proc. Natl. Acad. Sci. USA* **1999**, *96*, 2019–2024.
(29) Bachmann, A.; Wildemann, D.; Praetorius, F.; Fischer, G.; Kiefhaber, T. Mapping backbone and side-chain interactions in the transition state of a coupled protein folding and binding reaction, *Proc. Nat. Acad. Sci. USA* **2011**, *108*, 3952–3957.
(30) Dogan, J.; Gianni, S.; Jemth, P. The binding mechanisms of intrinsically disordered proteins, *Phys. Chem. Chem. Phys.* **2014**, *16*, 6323–6331.
(31) Luitz, M. P.; Bomblies, R.; Zacharias, M. Comparative Molecular Dynamics Analysis of RNase-S Complex Formation, *Biophys. J.* **2017**, *113*, 1466–1474.
(32) Liu, D.; Karanicolas, J.; Yu, C.; Zhang, Z.; Woolley, G. A. Site-specific incorporation of photoisomerizable azobenzene groups into ribonuclease S, *Bioorganic Med. Chem. Lett.* **1997**, *7*, 2677–2680.
(33) Hamachi, I.; Hiraoka, T.; Yamada, Y.; Shinkai, S. Photoswitching of the Enzymatic Activity of Semisynthetic Ribonuclease S Bearing Phenylazophenylalanine at a Specific Site, *Chem. Lett.* **1998**, pages 537–538.
(34) James, D.; Burns, D. C.; Woolley, G. Kinetic characterization of ribonuclease S mutants containing photoisomerizable phenylazophenylalanine residues, *Protein Eng. Des. Sel.* **2001**, *14*, 983–991.
(35) Kneissl, S.; Loveridge, E. J.; Williams, C.; Crump, M. P.; Allemann, R. K. Photocontrollable Peptide-Based Switches Target the Anti-Apoptotic Protein Bcl-x L, *ChemBioChem* **2008**, *9*, 3046–3054.
(36) Zhang, Z.; Burns, D. C.; Kumita, J. R.; Smart, O. S.; Woolley, G. A. A Water-Soluble Azobenzene Cross-Linker for Photocontrol of Peptide Conformation, *Bioconjugate Chem.* **2003**, *14*, 824–829.
(37) The PyMOL Molecular Graphics System, Version 1.8, Schrödinger, LLC., *Schrödinger, LLC* **2015**.
(38) Boerema, D. J.; Tereshko, V. A.; Kent, S. B. H. Total synthesis by modern chemical ligation methods and high resolution (1.1 Å) x-ray structure of ribonuclease a, *Peptide Science* **2008**, *90*, 278–286.
(39) Stelea, S. D.; Keiderling, T. A. Pretransitional Structural Changes in the Thermal Denaturation of Ribonuclease S and S Protein, *Biophys. J.* **2002**, *83*, 2259–2269.
(40) Dice, J. F.; Chiang, H.-l.; Spencer, E. P.; Backer, J. M. Regulation of Catabolism of Microinjected Ribonuclease A, *J. Biol. Chem.* **1986**, *261*, 6853–6859.
(41) Dice, J. F. Microinjected ribonuclease A as a probe for lysosomal pathways of intracellular protein degradation, *J. Protein Chem.* **1988**, *7*, 115–127.
(42) Bagchi, S.; Boxer, S. G.; Fayer, M. D. Ribonuclease S dynamics measured using a nitrile label with 2D IR vibrational echo spectroscopy, *J. Phys. Chem. B* **2012**, *116*, 4034–4042.
(43) Dias, A. R.; Minas Da Piedade, M. E.; Martinho Simoes, J. A.; Simoni, J. A.; Teixeira, C.; Diogo, H. P.; Meng-Yan, Y.; Pilcher, G. Enthalpies of formation of cis-azobenzene and trans-azobenzene, *J. Chem. Thermodyn.* **1992**, *24*, 439–447.
(44) Das, M.; Rao, B. V.; Ghosh, S.; Varadarajan, R. Attempts to delineate the relative contributions of changes in hydrophobicity and packing to changes in stability of ribonuclease s mutants, *Biochemistry* **2005**, *44*, 5923–5930.
(45) Zanobini, C.; Bozovic, O.; Jankovic, B.; Koziol, K. L.; Johnson, P. J. M.; Hamm, P.; Gulzar, A.; Wolf, S.; Stock, G. Azidohomoalanine : A Minimally Invasive, Versatile, and Sensitive Infrared Label in Proteins To Study Ligand Binding, *J. Phys. Chem. B* **2018**, *122*, 10118–10112.
(46) Abraham, M. J.; Murtola, T.; Schulz, R.; Páll, S.; Smith, J. C.; Hess, B.; Lindah, E. Gromacs: High performance molecular simulations through multi-level parallelism from laptops to supercomputers, *SoftwareX* **2015**, *1-2*, 19–25.
(47) Best, R. B.; Zheng, W.; Mittal, J. Balanced protein-water interactions improve properties of disordered proteins and non-specific protein association., *J. Chem. Theory Comput.* **2014**, *10*, 5113–5124.
(48) Abascal, J. L. F.; Sanz, E.; García Fernández, R.; Vega, C. A potential model for the study of ices and amorphous water: TIP4P/Ice, *J. Chem. Phys.* **2005**, *122*, 234511.
(49) Sittel, F.; Filk, T.; Stock, G. Principal component analysis on a torus: Theory and application to protein dynamics, *J. Chem. Phys.* **2017**, *147*, 244101.

(50) Sittel, F.; Stock, G. Perspective: Identification of collective variables and metastable states of protein dynamics, *J. Chem. Phys.* **2018**, *149*, 150901.
(51) Sittel, F.; Stock, G. Robust density-based clustering to identify metastable conformational states of proteins, *J. Chem. Theory Comp.* **2016**, *12*, 2426–2435.
(52) Cooper, M. A. Label-free screening of bio-molecular interactions, *Anal. Bioanal. Chem.* **2003**, *377*, 834–842.
(53) Rosa, J. J.; Richards, F. M. Hydrogen Exchange from Identified Regions of the S-Protein Component of Ribonuclease as a Function of Temperature , pH , and the Binding of S-Peptide, *J. Mol. Biol.* **1981**, *145*, 835–851.
(54) Labhardt, A. M. Kinetic circular dichroism shows that the S-peptide a-helix of ribonuclease S unfolds fast and refolds slowly, *Proc Natl Acad. Sci, USA* **1984**, *81*, 7674–7678.
(55) Cowgill, R. W. Fluorescence and the structure of proteins. III. Effects of denaturation on fluorescence of insulin and ribonuclease, *Arch. Biochem. Biophys.* **1964**, *104*, 84–92.
(56) Noronha, M.; Lima, J. C.; Paci, E.; Santos, H.; Maçanita, A. L. Tracking local conformational changes of ribonuclease A using picosecond time-resolved fluorescence of the six tyrosine residues, *Biophys. J.* **2007**, *92*, 4401–4414.
(57) Kabsch, W.; Sander, C. Dictionary of protein secondary structure: Pattern recognition of hydrogen-bonded and geometrical features, *Biopolymers* **1983**, *22*, 2577–2637.
(58) Baakman, C.; Krieger, E.; Black, J.; Touw, W. G.; Vriend, G.; Joosten, R. P.; te Beek, T. A. A series of pdb-related databanks for everyday needs, *Nucleic Acids Research* **2014**, *43*, D364–D368.
(59) Schreiber, G.; Keating, A. E. Protein binding specificity versus promiscuity, *Curr. Opin. Struct. Biol.* **2011**, *21*, 50–61.